PETROGRAPHY AND CHEMISTRY OF LITHIC FRAGMENTS FROM THE APOLLO 17 73002 DRIVE TUBE.

S. N. Valencia[1-3], N. M. Curran[2-4], E. S. Bullock[5], C. M. Corrigan[6], B. A. Cohen[2], and the ANGSA Science Team. [1]University of Maryland, Department of Astronomy, College Park, MD 20742. [2]NASA Goddard Space Flight Center, Planetary Geology, Geophysics, and Geochemistry Laboratory, Greenbelt, MD 20771. [3]Center for Space Sciences and Technology, University of Maryland, Baltimore County, Baltimore, MD 21250. (sarah.n.valencia@nasa.gov). [4]The Catholic University of America, Washington D. C. 20064. [5]Geophysical Laboratory, The Carnegie Institution for Science, Washington D. C. 20015. [6]National Museum of Natural History, Smithsonian Institute, Washington D. C. 20560.

Introduction: Drive tube 73002 is the upper half of the ~70 cm double-drive tube 73001/73002 taken near Ballet crater during the Apollo 17 mission. The drive tube was sealed on the lunar surface and preserved for future analysis. The sample has recently become available for analysis through the Apollo Next Generation Sample Analysis (ANGSA) program.

The overarching goal of our team's work as part of the ANGSA consortium is to analyze the noble gas budget at varying depths within the 73002 core [1]. To place the noble gas analyses into geological context and maximize the scientific return of these samples, petrographical and chemical analyses are needed as supporting measurements. The work presented here is those supporting analyses.

Methods: Our team was allocated 21 lithic fragments (2 to 16 mg) from varying depths within the 73002 drive tube. Upon arrival at NASA Goddard Spaceflight Center, the samples used for this work were split into two portions. One portion was allocated for noble gas analysis and the other for petrography and major and minor element chemistry. Thin sections of samples were made at The Smithsonian Museum of Natural History for this portion of the work.

Petrographical and chemical information of the samples was collected by electron probe microanalysis (EPMA) including both spot analysis and quantitative compositional maps. Data was collected on the JEOL 8530F electron probes at The Smithsonian Museum of Natural History and The Carnegie Institution for Science, following the methods of [2,3] for the quantitative maps.

We collected quantitative compositional stage maps using wavelength-dispersive spectrometers (WDS). Maps were made of representative regions of the fragments for 14 common major and minor geological elements using JEOL and Probe for EPMA software. Maps were up to 575×530 pixels in size, and were collected using a 30 nA probe current, step and spot sizes of 1-2 µm, and count times of 100-300 msec, yielding analytical times of 15-30 hours.

Sample Results: Thus far, we have analyzed 14 of our allocated samples by EPMA. For each of these samples we have collected quantitative compositional

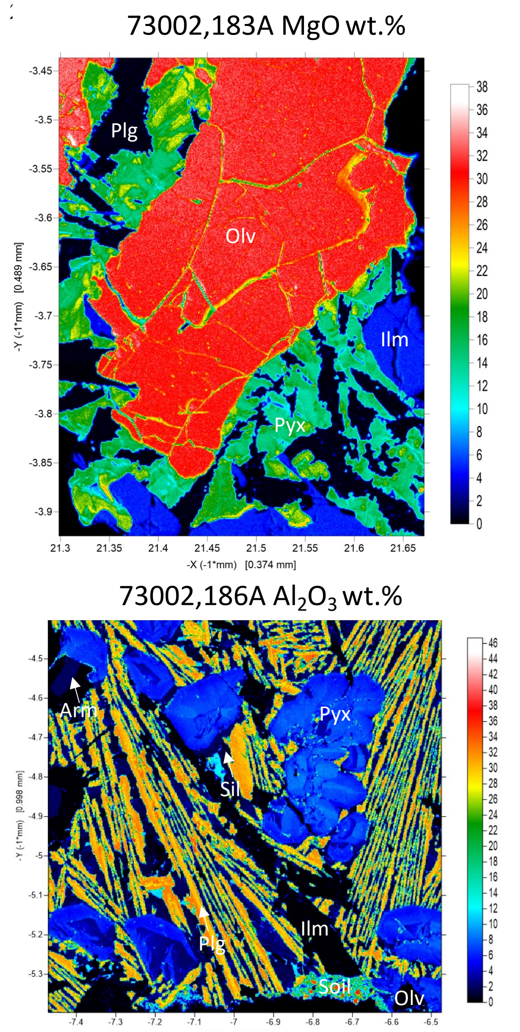

Figure 1. Quantitative compositional maps of basaltic fragments in 73002. Color scale corresponds to the amount of the oxide in the sample at each pixel. Each pixel in the image has a full 14-element chemical analysis. Arm = armalcolite, Ilm = ilmenite, Olv = olivine, Plg = plagioclase, Pyx = pyroxene, Sil = silica. **Top.** 73002,183A wt.% MgO. 73002,183A is dominated by a single olivine grain >500 µm long. Tabular pyroxene, plagioclase laths, and anhedral ilmenite grains are also major phases. **Bottom.** 73002,186A wt.% Al_2O_3. This fragment is dominated by subhedral pyroxene 200 × 300 µm in size, intergrown laths of plagioclase and acicular ilmenite, along with larger laths of ilmenite up to ~900 µm.

maps, as well as spot analysis of major minerals for comparison to the maps.

Basalts. We were allocated two basalt fragments (73002,183A [Fig. 1 top] and 73002,186A [Fig. 1 bottom]) with sufficient mass for splitting. Both basalts are high-Ti basalts. The major and minor mineralogy of the fragments includes ilmenite, clinopyroxene, plagioclase, olivine, and silica [4]. The fragments are texturally and chemically distinct from each other.

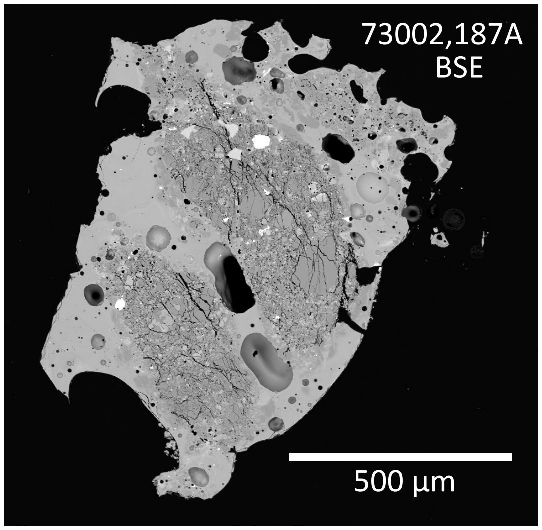

Figure 2. Agglutinitic fragment 73002,187A. the fragment contains abundant vesicles of varying sizes and an irregular boundary, along with FeNi metal fragments, indicative that this is an agglutinate.

Agglutanitic Fragment. One 3.45 mg fragment (73002,187A [Fig. 2]) is agglutanitic. This fragment has a highly irregular edge, abundant vesicles, and FeNi metal fragments up to ~50 µm in size. Some preserved regolith remains within the fragment. The regolith is dominated by plagioclase fragments, but olivine, sulfides, chromite, ilmenite, and phosphates also occur.

Norite. One 6.69 g fragment of norite (73002,189C) was allocated to our team. The fragment is almost exclusively composed of plagioclase, with minor orthopyroxene.

Breccias. The remaining nine fragments we have mapped are regolith, fragmental, or impact melt breccias. Breccia fragments range from 2.29 to 12.44 mg. A variety of textures occur within the samples, from the pyroxene and plagioclase fragment laden fragmental breccia 73002,184C to the vesicular impact melt breccia 73002,188C [Fig. 3]. The breccia samples are composed primarily of plagioclase, pyroxene, olivine, and silica, but are also host to minor to trace phosphates, sulfates, Ti-bearing minerals, Cr-bearing minerals and FeNi metal.

Future Work: Full chemical analysis for each of the fragments that underwent quantitative compositional mapping is in progress. Additionally, fragments from the lower drive tube 73001 are in preparation for chemical and petrographical analysis, as well as noble gas analysis.

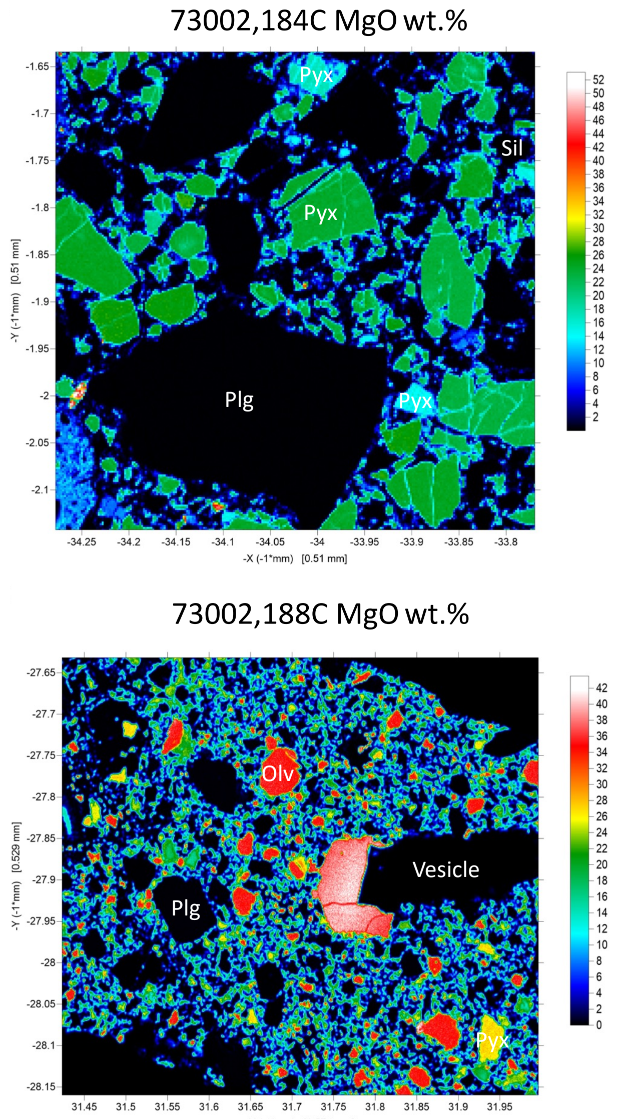

Figure 3. Quantitative compositional maps of breccia fragments in 73002. Color scale corresponds to the amount of the oxide in the sample at each pixel. Olv = olivine, Plg = plagioclase, Pyx = pyroxene, Sil = silica.

Acknowledgments: This work was funded through the NASA Apollo Next Generation Sample Analysis program. We thank Tim McCoy for making thin sections. Portions of this work were supported by NASA under award number 80GSFC21M0002.

References: [1] Curren N. M., et al. (2021) *LPSC 52*, Abstract #1592. [2] Carpenter P. C., et al. (2013) *LPSC 44*, Abstract #1827. [3] Donvoan J. J., et al. (2021) *Am. Min.* 106, 1717-1735. [4] Valencia S. V., et al. (2022) *LPSC 53*, Abstract #2608.